

PAPER • OPEN ACCESS

## The research of unstable slope monitoring in complex working environment using GB - SAR

To cite this article: Xiao Zhou *et al* 2019 *IOP Conf. Ser.: Earth Environ. Sci.* **227** 062033

View the [article online](#) for updates and enhancements.

# The research of unstable slope monitoring in complex working environment using GB - SAR

Xiao Zhou<sup>1,2,4</sup>, Zhenming Li<sup>1</sup>, Changjun Li<sup>1</sup> and Cheng Xing<sup>3</sup>

<sup>1</sup> Academy of Military Science Institute of defense engineering, Beijing, China;

<sup>2</sup> Army Engineering University Institute of defense engineering, Nanjing, China;

<sup>3</sup> Wuhan University Institute of Surveying and Mapping, Wuhan, China.

<sup>4</sup> Email: zhouxiao9988@126.com

**Abstract.** In hydropower project construction, the slope instability threatens the construction personnel safety. The slope stability in the process of construction monitoring is one of the most important tasks of the construction safety. Due to the GB-SAR technology has a non-contact, high accuracy, high space-time resolution characteristics; it is used to monitor the construction of slope in this paper. A whole scene atmospheric correction method using PS atmospheric correction network is proposed in this paper, and applied to the monitoring experiment of high-risk slope in construction. Finally the effectiveness of GB-SAR technique in complex engineering monitoring is verified by analyzing the different types of slope monitoring results.

## 1. Introduction

Ground-based SAR, which can accurately monitor target deformation in small area[1], has the characteristics of not containing space baseline, short sampling period, and high spatial resolution compared with the satellite-carried and plane-carried SAR. In the last nearly ten years, the researchers have conducted a mass of ground-based SAR application studies for glaciers[2], volcanoes[3,4], buildings[5-7], dams[8], landslides[9-12], and mine areas[13], with the result that the measuring accuracy of the technology are greatly influenced by atmospheric disturbances in the observation environment, and the atmospheric disturbances phase is often greater than the target deformation phase in the interferometric phase, which need to be corrected atmospherically choosing a suitable correction method for atmospheric disturbance phase.

Currently, there are two types of methods commonly used for GB-SAR atmospheric correction. The first type of methods uses the atmospheric factors of the environment, such as temperature, humidity and pressure to estimate the atmospheric impacts in the interferometric phase based on empirical model, and performs atmospheric correction[14]. The correction accuracy of such methods is influenced by the accuracy of both the model and the atmospheric factor measurements, and therefore is usually low. Another is to build relationship equation between atmospheric influence and the distance between the radar and the target (or the target's height information), using the stable targets at different position in the observation environment for atmospheric disturbance value, then solve the relationship equation for atmospheric correction of the targets in the different position[15-21]. The correction accuracy of this method, which is influenced by number, distribution, extraction accuracy of the stable points, has higher correction accuracy with small observation range, gentle atmospheric change in the environment, and obvious stable targets in the observation scene[22,23].



However, such atmospheric correction method based on the stable points cannot be effectively used under the situation of complex weather change, wide observation range (such as slope in construction), and unobvious stable targets in the observation scene. Unfortunately, there is no related research report about GB - SAR atmospheric correction method suitable for this condition.

This paper firstly introduces the GB - SAR atmospheric correction model and method based on the stable points, and proposes a new method for atmospheric correction using building PS atmospheric correction network, which aims at overcoming the shortcomings of the traditional correction methods. Then the method is applied to the deformation monitoring experiment of slope in construction using GB - SAR and comparison is made between such new method and traditional correction method based on the experimental data. The proposed method is verified effective taking the results of the measuring robot into consideration. Finally the stability of slope is analyzed using GB-SAR data.

## 2. GB - SAR atmospheric correction model and method

### 2.1. The atmospheric correction model based on the stable points

GB-SAR can obtain the interferometric phase of target which is mainly influenced by target deformation within the time of two observations as well as the atmospheric disturbance and noise in the environment due to GB-SAR's no containing of space baseline and shorter observation cycle time with interferometry technique, the relationship is as follows:

$$\phi^w = \phi_{atm} + \phi_{disp} + \phi_{noise} - 2n\pi \quad (1)$$

The noise effect  $\phi_{noise}$  can be weakened by selecting the points of high correlation and filter processing, and the weakened noise phase is negligible compared with  $\phi_{disp}$  and  $\phi_{atm}$ , thus eliminating atmospheric disturbance phase of GB-SAR interferometric phase to obtain the target deformation phase, then the deformation value of target in the radar line of sight is available. Similarly, the deformation phase of the fixed stable point in the observation scene is zero, which determines that its interference phase can be approximate to the atmospheric disturbance phase.

Atmospheric correction method based on the stable points presumes that atmospheric disturbances affect in the observation scene  $\phi_{atm}$  has a relationship with the distance between the target and the radar  $r$ , and the atmospheric phase obtained by the stable point as well as the distance between the point and radar is used to calculate the coefficient in (2) so as to make atmospheric correction for the targets in different location.

$$\phi_{atm} = a \bullet r^2 + b \bullet r \quad (2)$$

In the equation,  $r$  represents the distance between the target and the radar,  $\phi_{atm}$  represents atmospheric disturbances affect value in  $r$ , and  $a$ ,  $b$  are the equation coefficients.

### 2.2. The correction method based on PS atmospheric correction network

When using stable points for atmospheric correction, there is need to accurately select the known stable points in the observation scene to calculate accurate equation coefficient. In practice, however, accurate stable points in the scene are unavailable sometimes because of a shortage of available external information. Moreover a large number of stable points distributed evenly are needed to accurately estimate the atmospheric disturbances value in different position when the environment is more complex in the observation scene. The factors above lead to the result that traditional atmospheric correction method can't be effectively used.

In order to overcome the shortcomings of the traditional atmospheric correction, this paper proposes an atmospheric correction method based on PS atmospheric correction network. Firstly, extract the stable points in the observation area using PS technology, and make a statistical analysis of the stable point phase. Next, filter stable points in the scene and set distance threshold to build

Delaunay triangulation network for PS atmospheric correction. Finally, make atmospheric correction of target points using the PS atmospheric network. Notably, the target point in the network is corrected using the vertex of the triangle area where the point is located, whereas the target point outside the network is corrected using the closest three PS points.

The steps used to build the PS atmospheric correction network are as follows:

Since PS points have the characteristics of strong scattering and high stability, multiple threshold method which combines amplitude threshold, correlation coefficient threshold and amplitude discrete index threshold together is used for a screening of the PS points in the observation scene step by step, and the screening procedures are as follows:

1) Calculate the correlation coefficient of each pixel in each image of M time sequence GB - SAR interferograms images sequence, and build time sequence with the correlation coefficient of each pixel  $\gamma_m (m = 1, 2, \dots, M)$ .

2) Calculate the average of correlation coefficient of the pixel building the time sequence

$$\bar{\gamma} = \frac{\sum_{m=1}^M \gamma_m}{M}$$

3) Set correlation coefficient threshold value, select  $\gamma_m (i, j) (m = 1, 2, \dots, M) > \bar{\gamma}$  PS points as candidate PSC1.

4) Compute PSC1 amplitude dispersion index  $D_A$  in the time sequence GB - SAR interferograms.

5) Set reasonable amplitude discrete index threshold  $T_{DA}$ , pick  $D_A < T_{DA}$  pixel as PS candidate PSC2.

6) Calculate the amplitude sequence  $m_A$  of time sequenced GB - SAR image.

7) Set the amplitude threshold  $T_{mA}$ , screen  $m_A > T_{mA}$  PSC2 to obtain PSC3.

Then screen PSC3 points and build PS network used for the whole scene atmospheric correction, the steps are as follows:

1) Set the side length threshold used for building PS network and filter the points distributed densely in PSC3.

2) Estimate the atmospheric disturbance value of PS points according to the formula (4) (5).

3) Eliminate atmospheric disturbance phase calculated in (2) to PS points.

4) Make a statistical analysis of the residual phase of PS points, set residual error threshold value, delete PS points whose residual phase do not conform to the normal distribution and averages are more than the threshold, then return to step (2), until the selected PS points meet the requirements.

### 3. Slope monitoring experiment

Our study group carried out a deformation monitoring experiment on the excavation slope of a hydropower station during construction in Yunnan province, China. The surface of excavation slope which had landslide before the experiment is reinforced with concrete subsequently. In order to ensure the construction safety of the slope after reinforcement, stability monitoring of the reinforced slope and its surrounding area is carried out, and thus we make continuous measurement of two slopes to monitor the stability of the slopes after reinforcement under the influence of construction surroundings using GB - SAR technology. The observation platform where GB-SAR is erected is located on the other side of the monitored slope, with equal altitude to the bottom of the slope. The radar's line of sight is adjusted approximate parallel with the main sliding direction of the slope according to the initial monitoring information of the slope, and therefore the radar monitoring value can be regarded as the value of the slope deformation.

The radar signal power of observation scene corresponding with the overall slopes is shown in figure 1, 2, and the construction slope as well as the surrounding area is in the yellow box in figure.

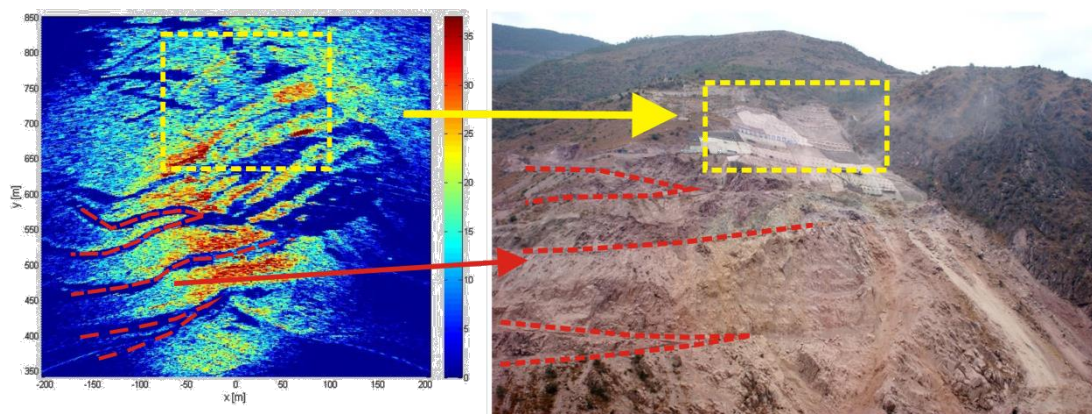


**Figure 1.** The relation map between Slope 1 area and Radar signal power.

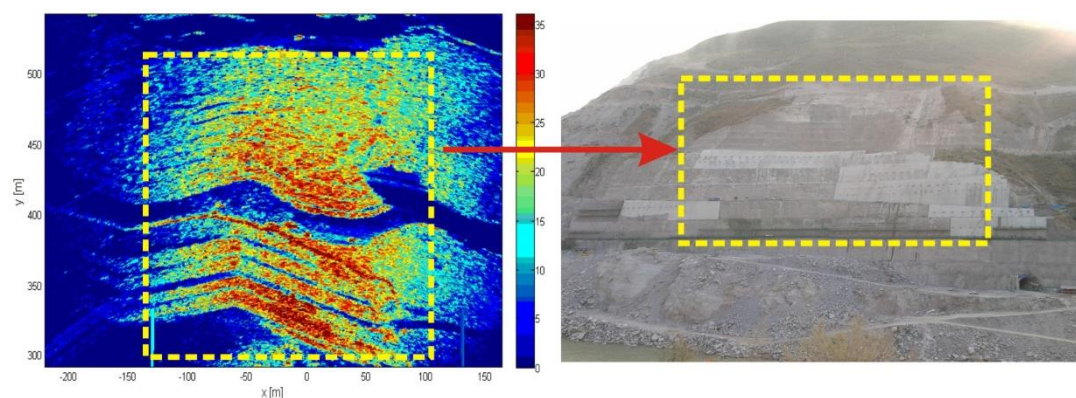


**Figure 2.** The relation map between Slope 2 area and Radar signal power.

#### 4. Atmospheric disturbance analysis

The correlation coefficient threshold is set to 0.9 when we select PS point, and amplitude of discrete index is set to 0.15, amplitude intensity is set to 25 dB. Finally the 2712 PSC3 points are selected for the analysis of the atmospheric correction. Then 18 PS points are selected to build atmospheric correction network according to the distance threshold value which is set to 35m, and in order to test the reliability of meteorological influence value counted by PS points, we choose five peripheral PS points for residual phase analysis; the PS residual phase values after filtering are shown in figure 3. It shows that the phase residual value corrected by PS point's meteorological correction method can be controlled within 0.5 mm, using which it could estimated the meteorological influence value accurately and meet the need of detecting submillimeter level deformation of target. To verify the reliability of the method proposed in this paper, we select three target points in different distance of the observation scene, using the proposed method and the traditional method for meteorological correction respectively. Since there is no other external information to determine the stable points in the mountain when choosing points for meteorological correction, we choose stable points for meteorological correction in the bottom of the mountain, considering it is relatively stable. Original deformation of the target, deformation after traditional meteorological correction, and target deformation after PS network correction are shown in figure 4, 5, 6, respectively. Figure 4 illustrates that the construction environment has a greater impact on the radar measurements, and the deformation tendency of the original measurements has obvious correlation with meteorological change, with the meteorological impact value of 12 mm; It is knowable from figure 5, 6 that in the period of severe atmospheric disturbance (around noon), atmospheric correction method of point selection can't effectively weaken the atmospheric disturbance, and the atmospheric impact value still

reaches 3 mm. However the meteorological impact value after correction with PS network can be effectively controlled within 1 mm, reflecting target deformation information more accurately.

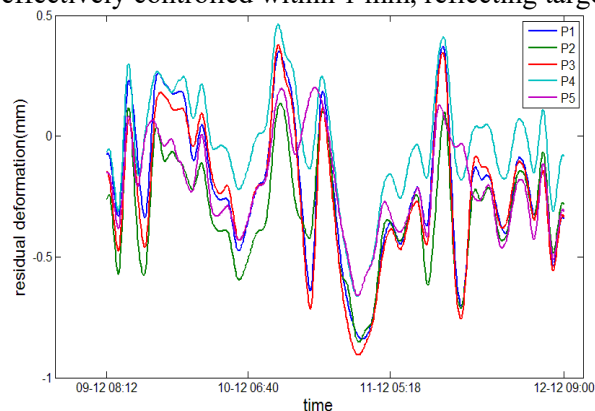


**Figure 3.** The residual deformation figure of PS.

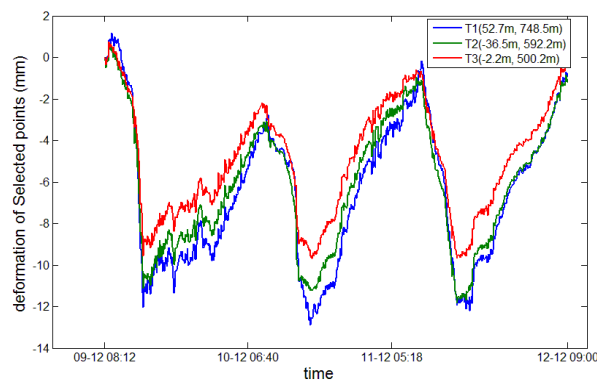


**Figure 4.** the original deformation figure of targets.

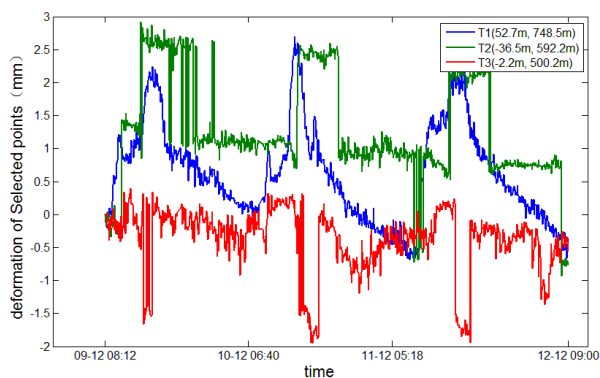


**Figure 5.** The deformation figure after correction correction using choosing point method.

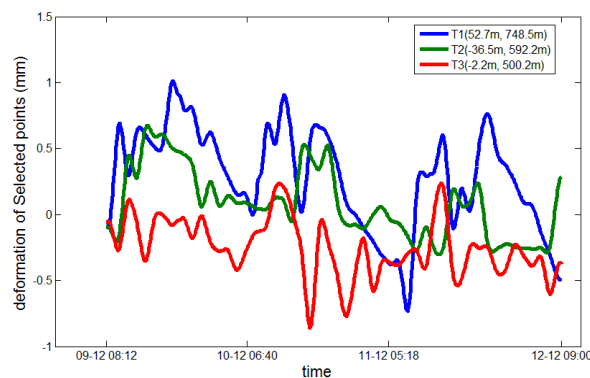


**Figure 6.** The deformation figure after using PS network method.

### 5. Slope deformation analysis

The target points of observation scene are corrected meteorologically using PS meteorological correction network and the final whole slope deformation is shown in figure 7 (The positive represents the reverse of the radar's line of sight). Figure 7 illustrates that during the period of GB-SAR's monitoring there are three abnormal areas whose deformation values are greater compared with the nearby targets, two in which are in the region of excavation slope 1. Other areas of the excavation slope 1 have smaller deformation, and the top of the slope 1 has larger deformation relative to the central region, but the cumulative deformation values are not more than 1.5 mm. choosing one characteristic point respectively from the abnormal area 1, 2, and the central region of excavation slope 1 and observing the deformation feature, the deformation values of the characteristic points are shown in figure 8. The figure 8 shows that target points in the abnormal area 1 and 2 present significant declines, and the deformation values reach 4 mm and 2.5 mm respectively, which indicates the landslide danger. In order to ensure the construction safety and inspect GB - SAR measurement results, we set temporary monitoring point L13 additionally around the abnormal area 2, and monitor four points including L13, a monitoring point around abnormal area 1 and two points in other parts of the slope 1 using total station. The position of abnormal area and monitoring points in excavation slope 1 is shown in figure 9, and the target in abnormal area presents a significant downward trend and deformation reaches up to 4 mm, which accord with GB - SAR measurement results and indicate the need for reinforcement; In other parts of excavation slope 1 the deformation trend is gentle, and

central area displacement of the slope 1 is less than 1 mm. The deformation of the top is larger relative to the central of slope 1, and its displacement in the radar's line of sight is about 1.8 mm, which is consistent with the radar measurement results. GB-SAR measurement results can accurately reflect the deformation trend in different parts of the slope 1 according to the comparative analysis of the measurement results of total station.

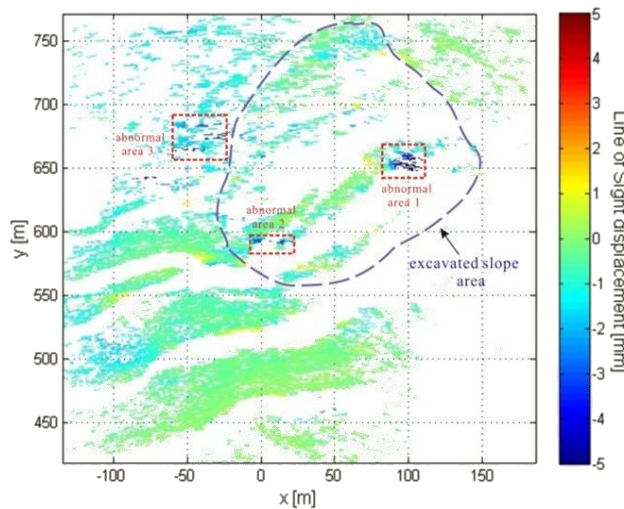


**Figure 7.** The deformation figure of the whole slop1.

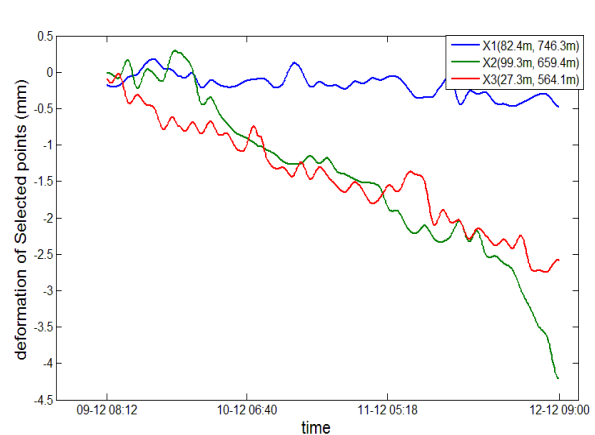


**Figure 8.** The deformation of the characteristic points.



**Figure 9.** The live-action photo of the excavated slope 1.

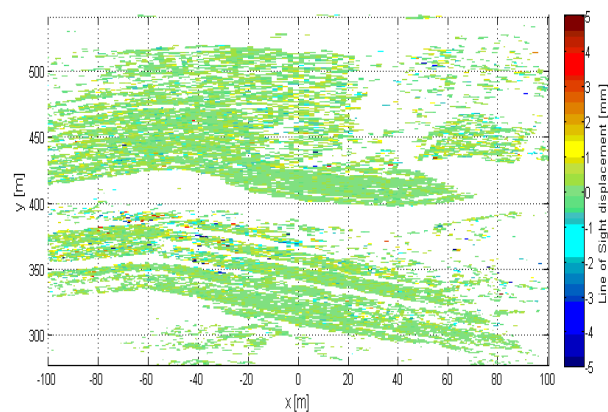


**Figure 10.** The deformation figure of the whole slop2.

The figure 10 shows that the deformation of reinforced slope 2 is small in the monitoring period. The overall shape variable is less than 0.5 mm, so it can be proved the slope structure is very stable. There are some abnormal deformation points on the upper part of the bottom slope, near the top and bottom slope. The emergence of these points mainly is because of in the process of monitoring, some transportation vehicles appeared on the road which is in the middle the top and bottom slope. The radar echo phase of the special position on the slope is influenced by the vehicle, produce phase wrapped, and then this part of slope shows abnormal deformation.

## 6. Conclusions

This paper discusses the GB - SAR atmospheric correction model and method, proposing PS selection of multiple thresholds as well as the method and steps in detail of building PS atmospheric correction network, and applied the method to the practice of slope monitoring. The GB - SAR atmospheric disturbances analysis shows that measurement accuracy of GB - SAR is seriously affected by atmospheric disturbances in complex environment, and the atmospheric impact value can be up to 12 mm when influenced by factors in the environment such as dust, vapor in the monitoring experiment of slope in construction. In the period of severe atmospheric disturbance (around noon), atmospheric correction method of point selection can't effectively weaken the atmospheric disturbance, and the atmospheric residual phase sometimes reaches 3 mm, which is greater than the target deformation phase and makes the atmospheric correction results unable to accurately reflect the real deformation of target. PS selection method of multiple thresholds combined with PS atmospheric residual statistical analysis make it possible to select the optimal stable point in the observation scene having no obvious prior stable point, and setting the appropriate distance threshold and selecting PS distributed evenly to build atmospheric correction network will control the impact value within 1 mm. Finally, the results of slope monitoring experiment show that measurements corrected with the method proposed in this paper accurately detect three abnormal deformation areas of the measured slope, which is basically consistent with the deformation trend detected by measuring robots so as to verify the reliability of the atmospheric correction method proposed in this paper and the feasibility of GB-SAR in excavated slope monitoring.

## Acknowledgements

This work was supported by the CRSRI Open Research Program (Program SN: CKWV2017518/KY), Hubei Provincial Natural Science Foundation (NO. 2017CFB654).

## References

- [1] O. Monserrat M C G L 2014 A review of ground-based SAR interferometry for deformation measurement [J] *ISPRS Journal of Photogrammetry and Remote Sensing* **93** 40-48
- [2] Han H, Lee H 2011 Motion of Campbell glacier, East Antarctica, observed by satellite and ground-based interferometric synthetic aperture radar [C] *Seoul, Korea, Republic of: IEEE Computer Society*
- [3] Sabine Rödelaspergera, Matthias Beckera, Carl Gersteneckera, et al. 2010 Digital elevation model with the ground-based SAR IBIS-L as basis for volcanic deformation monitoring [J] *Journal of Geodynamics* **49** 241-246
- [4] Noferini L, Mecatti D, Macaluso G, et al. 2009 A high speed microwave interferometer used for monitoring Stromboli volcano [C] *Cape Town, South africa: Institute of Electrical and Electronics Engineers Inc.*
- [5] Gentile C, Bernardini G 2010 An interferometric radar for non-contact measurement of deflections on civil engineering structures: Laboratory and full-scale tests [J] *Structure and Infrastructure Engineering* **6(5)** 521-534
- [6] Pieraccini, M., et al. 2004 2004 High-speed CW step-frequency coherent radar for dynamic monitoring of civil engineering structures *Electronics Letters* **14(40)** 907-908
- [7] Antonello, G., et al. 2003 A ground-based interferometer for the safety monitoring of landslides and structural deformations. in *Geoscience and Remote Sensing Symposium, IGARSS'03. Proceedings. 2003 IEEE International NEW YORK: IEEE*
- [8] Alba M, Bernardini G, Giussani A, et al. 2008 Measurement of dam deformations by terrestrial interferometric techniques [J] *The International Archives of the Photogrammetry, Remote Sensing and Spatial Information Sciences* **37** 133-139
- [9] Takahashi K, Mecatti D, Dei D, et al. 2012 Landslide observation by ground-based SAR interferometry [C] *Munich, Germany: Institute of Electrical and Electronics Engineers Inc.*
- [10] Bozzano F, Cipriani I, Mazzanti P, et al. 2011 Displacement patterns of a landslide affected by

- human activities: insights from ground-based InSAR monitoring [J] *NATURAL HAZARDS* **59(3)** 1377-1396
- [11] Casagli N, Catani F, Del Ventisette C, et al. 2010 Monitoring, prediction, and early warning using ground-based radar interferometry [J] *LANDSLIDES* **7(3)** 291-301
- [12] Tofani, V., et al. 2014 Integration of remote sensing techniques for intensity zonation within a landslide area: A case study in the Northern Apennines, Italy *Remote Sensing* **6(2)** 907-924
- [13] Luca Pipia A A, Xavier Fabregas, Jordi. J. Mallorqui, et al. 2007 Mining Induced Subsidence Monitoring in Urban Areas with a Ground-Based SA [J] *Urban Remote Sensing Joint Event*.
- [14] Iannini L, Guarnieri A M 2011 Atmospheric Phase Screen in Ground-Based Radar: Statistics and Compensation [J] *GEOSCIENCE AND REMOTE SENSING LETTERS* **8(3)** 537-541
- [15] R Iglesias X F A A 2013 Atmospheric Phase Screen Compensation in Ground-Based SAR With a Multiple-Regression Model Over Mountainous Regions [J] *TRANSACTIONS ON GEOSCIENCE AND REMOTE SENSING*
- [16] Keith Morrisona, J.B.S.S. 2013 Ground-based C-band tomographic profiling of a conifer forest stand *International Journal of Remote sensing* **34(21)** 7838-7853
- [17] Xiang, Z., et al. 2011 Atmospheric disturbance correction in Ground-Based SAR differential interferometry. in Radar (Radar) 2011 *IEEE CIE International Conference on*
- [18] Fabregas X R I A 2012 A new approach for Atmospheric Phase Screen Compensation in Ground-Based SAR over areas with steep topography[Z]
- [19] Iwe H 2012 Ground based interferometric synthetic aperture radar for monitoring slowly moving surfaces[D]
- [20] Yigit E, Demirci S, Unal A, et al. 2012 Millimeter-wave Ground-based Synthetic Aperture Radar Imaging for Foreign Object Debris Detection: Experimental Studies at Short Ranges[J] *Journal of Infrared, Millimeter, and Terahertz Waves* **33(12)**1227-1238
- [21] X Zhou Y M X P 2013 Research on Atmospheric Disturbance Correction method of ground-based radar interferometry [J] *IOP Conference Series: Earth and Environmental Science* 17
- [22] Pipia L, Fabregas X, Aguasca A, et al. 2008 Atmospheric Artifact Compensation in Ground-Based DInSAR Applications [J] *Geoscience and Remote Sensing Letters, IEEE*. **5(1)** 88-92
- [23] J. van der Geer, J.A.J. Hanraads, R.A. Lupton 2000 The art of writing a scientific article *J. Sci. Commun.* **163** 51-59